



Research papers

Synergistic effects of temporal variations in flow and chemistry on colloid retention and remobilization in saturated porous media

Yerramilli Sai Rama Krishna^a, N. Seetha^{a,*}, S. Majid Hassanizadeh^{a,b,c}

^a Department of Civil Engineering, Indian Institute of Technology Hyderabad, Kandi, Sangareddy 502285, India

^b Stuttgart Center for Simulation Science (SIMTECH), Integrated Research Training Group SFB 1313, Stuttgart University, Germany

^c Department of Earth Sciences, Utrecht University, 3584, CB, Utrecht, the Netherlands

ARTICLE INFO

Keywords:

Colloids
Remobilization
Temporal variations
Flow
Chemistry
Porous media

ABSTRACT

Rapid infiltration due to rainfall events, groundwater pumping, and artificial recharge of groundwater result in temporal variations in both flow and chemistry in the subsurface and may lead to remobilization of retained colloids, thereby re-contaminating the groundwater resources. Many researchers have studied the effects of temporal variations in water velocity and in water chemistry separately. These variations, however, almost always occur simultaneously. To the best knowledge of the authors, there are no studies reported in the literature where the effect of simultaneous temporal variations in flow velocity and ionic strength on colloid release is investigated. One cannot assume that those effects can be simply superimposed. In fact, in this study, we show that these effects are not simply additive. We have performed eight sets of saturated column experiments on the effects of temporal variations in flow velocity alone and simultaneous temporal variations in flow velocity and ionic strength on retention and remobilization of colloids. Temporal increases in average water velocity caused an instantaneous spike release of colloids in the measured breakthrough curve, with the time to peak coinciding with the instant of velocity increase. Further, the effect of temporal variations in average water velocity on remobilization of deposited colloids is ionic-strength dependent. The simultaneous temporal increases in flow and decreases in ionic strength caused a spike release of colloids followed by long tails. The release curve for every step-change in velocity and ionic strength was unimodal for deposition ionic strengths of 100 and 10 mM, with the peak coinciding with the instant of arrival of ionic strength front at the column outlet. However, the release curve was bimodal for deposition ionic strengths of 50 and 25 mM. There, the first instantaneous spike coincided with the instant of increase in flow velocity, and the second delayed one coincided with the passage of the ionic strength front. Temporal variations in both flow and ionic strength released more colloids in the effluent than when only ionic-strength or only flow velocity was varied. This is due to the combined effects of greater hydrodynamic torque exerted on attached particles together with smaller adhesive torque.

1. Introduction

Groundwater is a major source of drinking water for millions of people worldwide, and contributes to significant quantity of agricultural and industrial water (Carrard et al., 2019; Ramesh and Elango, 2012; Singh et al., 2006). However, alarming increase in groundwater contamination poses a significant threat to human health and environment (Karunanidhi et al., 2021; Lapworth et al., 2012; Li et al., 2021). Several colloidal contaminants such as pathogenic microorganisms, microplastics, and engineered nanoparticles enter the subsurface through various human activities, such as improper maintenance of

septic tanks, leakages from sewer lines, and sewage disposal on land without proper treatment (Akhtar et al., 2021; Mishra et al., 2019; Mukhopadhyay et al., 2022). Soil acts as a filter by retaining a fraction of the infiltrated colloids, thereby partially decontaminating the infiltrated water. However, temporal variations in flow and chemistry of subsurface due to precipitation events, groundwater pumping, and artificial recharge of groundwater may lead to remobilization of previously deposited colloids from soil surfaces, leading to recontamination of the groundwater resources (Auset et al., 2005; Bradford and Kim, 2012; Bradford et al., 2015; Lenhart and Sayers, 2003; Tosco et al., 2009; Torkzaban et al., 2010; Torkzaban et al., 2015; Zhuang et al., 2007).

* Corresponding author.

E-mail address: seetha@ce.iith.ac.in (N. Seetha).

<https://doi.org/10.1016/j.jhydrol.2024.132144>

Received 10 June 2024; Received in revised form 14 September 2024; Accepted 22 September 2024

Available online 11 October 2024

0022-1694/© 2024 Elsevier B.V. All rights reserved, including those for text and data mining, AI training, and similar technologies.

Hence, it is essential to understand the mechanisms of colloid retention and release during temporal variations in flow and chemistry to assess the groundwater contamination potential. So far, effects of such variations have been studied separately, as explained below.

A few studies investigated the effect of temporal variations in flow velocity on remobilization of deposited colloids in saturated porous media (Auset et al., 2005; Bergendahl and Grasso, 2000; Carstens et al., 2017; El Farhan et al., 2000; Kermani et al., 2020; Nishad et al., 2021; Torkzaban et al., 2015; Wang et al., 2016; Zhang et al., 2012, 2015). The above studies observed a spike release of colloids, coinciding with the increase in flow velocity, followed by a long tail (Bergendahl and Grasso, 2000; El Farhan et al., 2000; Torkzaban et al., 2015; Zhang et al., 2015). This is due to greater hydrodynamic drag force acting on deposited colloids at larger velocities, which remobilizes them. However, it was observed that only a fraction of deposited colloids was released during every step-increase in velocity, and the amount of release depended on the magnitude of velocity change (Bergendahl and Grasso, 2000; El Farhan et al., 2000; Torkzaban et al., 2015). The fractional release of colloids was attributed to the spatial variability of adhesive and hydrodynamic torques due to charge heterogeneity and roughness of soil grains, presence of flow stagnation zones, and presence of strained colloids (Bradford and Bettahar, 2006; Bradford and Torkzaban, 2013; Du et al., 2013; Johnson et al., 2007; Kermani et al., 2020). The above findings were supported by the micromodel investigations of Zhang et al. (2015) and Nishad et al. (2021). Additionally, the attached colloids on pore wall were observed to translate during flow interruption and were released when the flow was resumed (Carstens et al., 2017).

The effect of temporal variations in ionic strength on remobilization of deposited colloids has been studied by several researchers through column-scale and pore-scale experiments (Bradford and Kim, 2012; Bradford et al., 2015; Krishna et al., 2022; Lenhart and Saiers, 2003; Li et al., 2017; Liang et al., 2020; Nishad et al., 2021; Nocito and Tobiason, 1996; Pazmino et al., 2014; Sadeghi et al., 2011; Shen et al., 2007, 2012, 2015, 2018; Torkzaban and Bradford, 2016; Torkzaban et al., 2010; Tosco et al., 2009; Wang et al., 2019, 2020; Zhou et al., 2011). The above studies observed that colloid release curve during step-decreases in ionic strength is characterized by sharp peaks followed by extended tailing and the time to peak coincides with the time of arrival of ionic strength front at the outlet of the column (Bradford and Kim, 2012; Bradford et al., 2015; Krishna et al., 2022; Lenhart and Saiers, 2003; Torkzaban et al., 2010; Tosco et al., 2009). Decrease of the ionic strength results in changes in interaction energy which leads to the release of deposited colloids. Decrease in ionic strength increases the repulsion between a colloid and collector, resulting in decreased primary and secondary minima depths, thereby causing detachment of deposited colloids (Fang et al., 2013; Zhou et al., 2011). Also, the mass of colloids released was found to be greater when the colloids were deposited at high ionic strengths (Krishna et al., 2022; Li et al., 2017; Nishad et al., 2021; Nocito and Tobiason, 1996). However, the fraction of deposited colloids that was released decreased, when the colloids were deposited at higher ionic strengths (Krishna et al., 2022; Lenhart and Saiers, 2003; Pazmino et al., 2014; Torkzaban et al., 2010). Though many studies observed colloid release during every step-decrease in ionic strength (Bradford et al., 2015; Krishna et al., 2022; Lenhart and Saiers, 2003; Wang et al., 2020), Tosco et al. (2009) observed colloid release only when the ionic strength was decreased to 0 mM or when the pH was increased to 11. Surface roughness and charge heterogeneity of sand grains were found to play important roles in colloid remobilization. The colloids deposited at the top of roughness elements will be released due to the elimination of finite depth of primary minimum upon reduction in ionic strength (Bradford et al., 2015; Torkzaban and Bradford, 2016; Li et al., 2017; Liang et al., 2020; Shen et al., 2012, Wang et al., 2019, 2020). However, colloids are found to be irreversibly retained in the concave locations between the roughness asperities and are not susceptible to release with reduction in ionic strength (Liang et al., 2020). Further, Nishad et al. (2021) and Bhuvankar et al. (2022) reported

re-deposition of released colloidal clusters in the downstream regions resulting in pore clogging.

The above studies focused on the remobilization of colloids due to temporal variations in either flow velocity or ionic strength. However, infiltration due to rain events and agricultural activities affects both velocity and chemistry of the underlying groundwater. Rapid infiltration of rainwater may cause the groundwater velocity to increase and ionic strength to decrease. Colloids already deposited on the surface of the soil grains may get remobilized due to these perturbations, leading to recontamination of groundwater. To the best knowledge of the authors, no studies in the literature investigated the effects of simultaneous temporal variations in flow velocity and ionic strength on remobilization of deposited colloids. One cannot assume that the effect of temporal changes in water velocity and chemistry can be simply superimposed. In fact, as there are threshold values in flow velocity and in ionic strength beyond which remobilization may occur, we expect such temporal changes to influence each other's effect on colloid remobilization. In our previous study (Krishna et al., 2022), we investigated the effect of temporal variations in ionic strength on colloid release in a saturated porous medium experimentally and numerically. We found that there exists a critical ionic strength between 10 and 1 mM, below which the colloid release was significant. In the current study, for the same physicochemical conditions as in Krishna et al. (2022), we assess the effects of a) temporal variations in flow velocity alone, and b) simultaneous temporal variations in flow velocity and ionic strength on colloid retention and remobilization in saturated porous media. A total of eight sets of column experiments were performed in this study, four experiments for temporal variations in flow alone and four for simultaneous temporal variations in flow velocity and ionic strength.

2. Materials and methods

2.1. Sand, colloids, and background electrolyte

River sand with grain size between 425 and 600 μm was used as the representative aquifer material for performing column experiments. Before packing into the column, the sand was washed with hydrochloric acid to eliminate metal oxides and other organic impurities as explained in Krishna et al. (2022). Carboxylate-modified latex (CML) beads of size 1 μm , purchased from Thermo Fisher Scientific Pvt. Ltd., were used as the model colloids in this study. NaCl was used for preparing the background electrolyte at six different ionic strengths of 100, 50, 25, 10, 1, and 0.1 mM, in which CML colloids were suspended. The injection concentration of CML colloids for all experiments was 7.3×10^7 no./mL. The pH of the background electrolyte was maintained at neutral by using 0.1 N HCl and 0.1 M NaOH. The zeta potentials of sand were measured to be $-13.08 (\pm 1.61)$, $-16.03 (\pm 3.35)$, $-20.03 (\pm 3.76)$, $-29.57 (\pm 2.42)$, $-30.36 (\pm 0.69)$, $-31.01 (\pm 1.82)$, and $-44.46 (\pm 2.96)$ mV at ionic strengths of 100, 50, 25, 10, 1, 0.1 and 0 mM, respectively. The corresponding zeta potentials of CML colloids were $-16.46 (\pm 0.39)$, $-41.16 (\pm 0.68)$, $-45.35 (\pm 1.06)$, $-48.95 (\pm 0.66)$, $-67.46 (\pm 0.96)$, $-78.66 (\pm 3.04)$, and $-84.15 (\pm 3.64)$ mV, respectively.

2.2. Column experiments

A cylindrical plexi-glass column with an inner diameter of 2.5 cm and a length of 15 cm was used for performing the column experiments. The column was placed vertically and wet-packed with sand. The bulk density and porosity of sand were determined to be 1.67 g/cm^3 and 0.37, respectively. A detailed description of the experimental setup is given in Krishna et al. (2022). Eight sets of column experiments were performed in this study (Tables 1 and 2): experiments 1–4 correspond to colloid transport and release behavior due to temporal variations in flow velocity while maintaining a constant ionic strength throughout the experiment (Table 1), and experiments 5–8 correspond to colloid transport and release behavior due to simultaneous temporal variations

Table 1

List of experiments on colloid remobilization due to temporal variations in average water velocity.

Experiment no.	Ionic Strength (mM)	Average water velocity (cm/min)			
		Stages 1 & 2	Stage 3		
			Step 1	Step 2	Step 3
1	100	0.55	2.75	5.5	11
2	50	0.55	2.75	5.5	11
3	25	0.55	2.75	5.5	11
4	10	0.55	2.75	5.5	11

in flow velocity and ionic strength (Table 2). The experimental procedure for performing each of the above experiments is described below.

The packed column was flushed with 10 pore volumes (PVs) of deionized (DI) water at an average water velocity of 0.55 cm/min (flow rate of 1 mL/min). Subsequently, a tracer experiment was conducted by passing an aqueous solution of 100 mM NaCl for 3 PVs, followed by flushing the column with DI water for another 3 PVs by maintaining the same average water velocity of 0.55 cm/min. Effluent samples were collected from the column outlet at regular intervals of 0.22 PVs and analyzed for NaCl concentration using an electrical conductivity meter. Following this, the column was equilibrated with 10 PVs of background electrolyte at the desired ionic strength and at an average water velocity of 0.55 cm/min. Finally, experiments were performed to investigate colloid transport. Each colloid transport experiment comprised of three stages: stages 1 & 2 investigated colloid transport at a constant average water velocity of 0.55 cm/min (flow rate of 1 mL/min) and at a desired ionic strength of 100, 50, 25, or 10 mM, whereas stage 3 corresponded to temporal variations in flow (and chemistry) due to a step increase in average water velocity without (or with) a simultaneous step decrease in ionic strength of the inflow solution. In stage 1, the colloidal suspension was injected into the column at a desired ionic strength at an average water velocity of 0.55 cm/min for 3 PVs, followed by stage 2 in which the flow of colloid-free background solution at the same average water velocity and ionic strength was continued for 3 PVs. Experiments 1–4 correspond to temporal variations in flow rate in stage 3, with each experiment having a different ionic strength as given in Table 1. For each of these experiments, the average water velocity was increased stepwise from 0.55 to 2.75, to 5.5, and to 11 cm/min without any change in the ionic strength. The corresponding flow rates are 5, 10, and 20 mL/min, respectively. After each step increase in average water velocity, the flow was continued for 3 PVs until the next step increase. It must be noted that the flow of water was never halted during any of the experiments. Effluent samples were collected from the column outlet at regular intervals of 0.22 PVs and analyzed for colloid concentration using a turbidity meter.

Experiments 5–8 correspond to simultaneous temporal variations in flow and chemistry in stage 3 with each experiment corresponding to a different initial ionic strength in stages 1 & 2 as given in Table 2. For each of these experiments, the average water velocity was increased in steps from 0.55 to 2.75, to 5.5, and to 11 cm/min in stage 3 with simultaneous step-decreases in ionic strength to 0 mM (DI water)

Table 2

List of experiments on colloid remobilization due to simultaneous temporal variations in flow and ionic strength.^a

Experiment no.	Stages 1 & 2		Stage 3											
	\bar{v}	IS	Step 1		Step 2		Step 3		Step 4		Step 5		Step 6	
			\bar{v}	IS	\bar{v}	IS	\bar{v}	IS	\bar{v}	IS	\bar{v}	IS	\bar{v}	IS
5	0.55	100	2.75	50	5.5	25	11	10	11	1	11	0.1	11	DI
6	0.55	50	2.75	25	5.5	10	11	1	11	0.1	11	DI	–	–
7	0.55	25	2.75	10	5.5	1	11	0.1	11	DI	–	–	–	–
8	0.55	10	2.75	1	5.5	0.1	11	DI	–	–	–	–	–	–

^a \bar{v} is the average water velocity in cm/min and IS is ionic strength in mM.

(Table 2). Each step change in average water velocity and ionic strength was applied for 3 PVs. After the average water velocity reached 11 cm/min in step 3, further temporal variations corresponded to only step decreases in ionic strength to 0 mM by maintaining the average water velocity at 11 cm/min (Table 2). Samples were collected from the column outlet at regular intervals of 0.22 PVs and colloid concentrations were measured using a turbidity meter. Each of the experiments (experiments 1–8) was repeated thrice to check the reproducibility of the results. The colloid breakthrough curve was then plotted as the normalized concentration of colloids in the effluent (c/c_0) versus PVs, where c_0 is the injection concentration of colloids.

At the end of each experiment, the sand inside the column was dissected into approximately 1 cm long sections to obtain the colloid retention profile. The mass of colloids retained on the sand in each section was then determined by first adding 20 mL of DI water to the sand followed by gentle shaking to release the colloids into the suspension (Wang et al., 2008; Xu et al., 2006). The suspension was then allowed to stand for 15 min for the sand particles to settle. After that, the colloid concentration in the supernatant was measured. Colloid retention profile is then plotted as the mass of colloids retained per mass of soil ($s \left[\frac{M}{M} \right]$) in each section versus distance from the column inlet.

3. Results and discussion

3.1. Colloid remobilization due to temporal variations in velocity

Figs. 1–4 show the colloid breakthrough curves for experiments 1–4, respectively. Fig. 5a and b show the colloid retention profiles at the end of stages 2 and 3 of experiments 1–4, respectively. The mass balance information for the above experiments along with the mass released during every step-increase in average water velocity in stage 3 are given in Table 3. Negligible release of attached colloids was observed when the ionic strength was 100 mM (experiment 1 and Fig. 1). This might be because of the large adhesive torque due to a deep primary minimum between the attached particles and soil grains at 100 mM ionic strength (Krishna et al., 2022 and Fig. S1). The hydrodynamic torque imparted by increased velocity could not overcome this adhesive torque. This is supported by Table 3 which shows that only 0.35 % of the injected mass was released in stage 3 of experiment 1.

A spike instantaneous release of colloids was observed with every step-increase in flow velocity at ionic strengths of 50 and 25 mM (experiments 2 and 3 and Figs. 2 and 3), with the release peak coinciding with the instant of velocity variation. This is due to the fact that at those lower values of ionic strength, the adhesive torque is not strong enough and the hydrodynamic torque acting on particles at larger velocities can remobilize attached colloids (Auset et al., 2005; Carstens et al., 2017; El Farhan et al., 2000; Kermani et al., 2020; Nishad et al., 2021; Zhang et al., 2015). Further, the release peak coinciding with the instant of velocity variation indicates an exponentially increasing release of colloidal mass with distance from the column inlet, with the greatest release occurring at the column outlet. Our preliminary modeling results

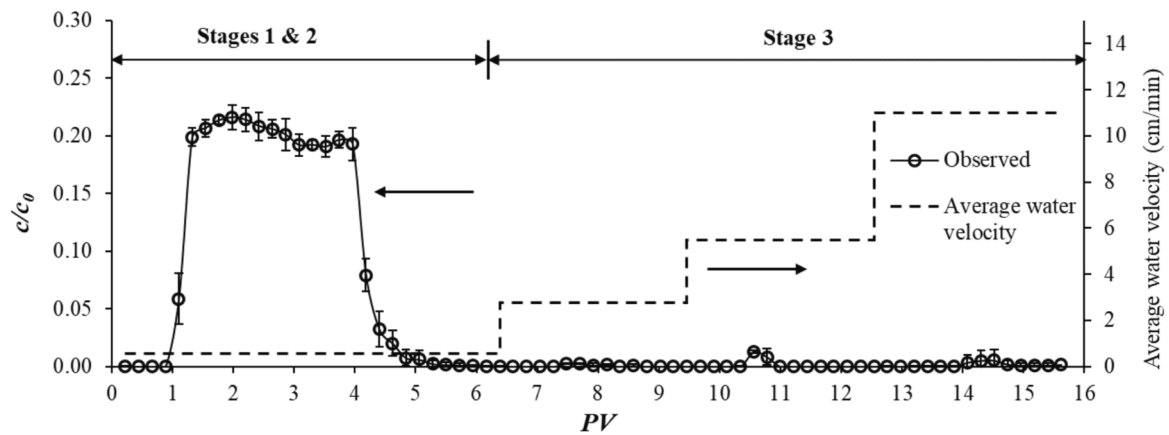


Fig. 1. Observed breakthrough curve of CML colloids for experiment 1. Average water velocity variation is shown on the secondary y-axis. Ionic strength was 100 mM.

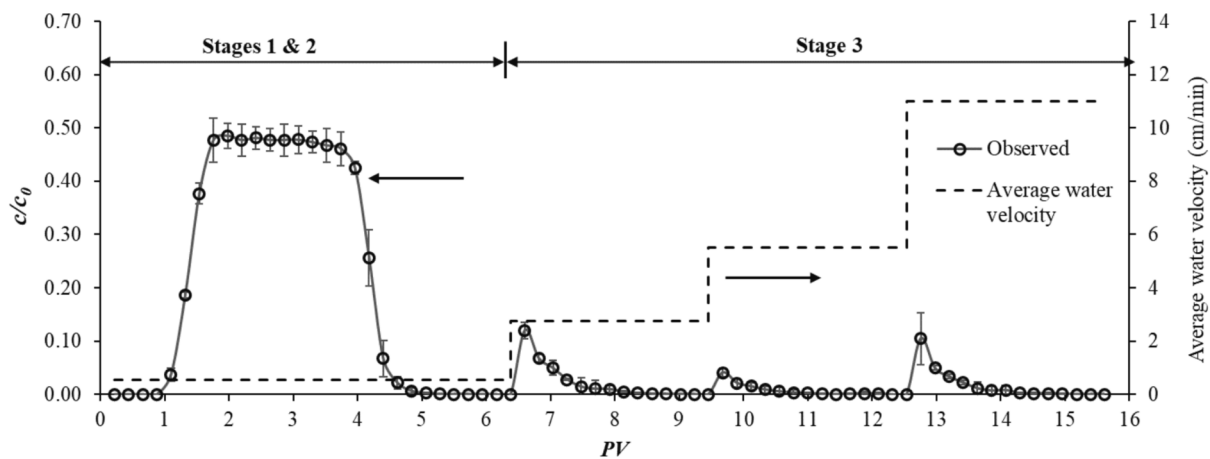


Fig. 2. Observed breakthrough curve of CML colloids for experiment 2. Average water velocity variation is shown on the secondary y-axis. Ionic strength was 50 mM.

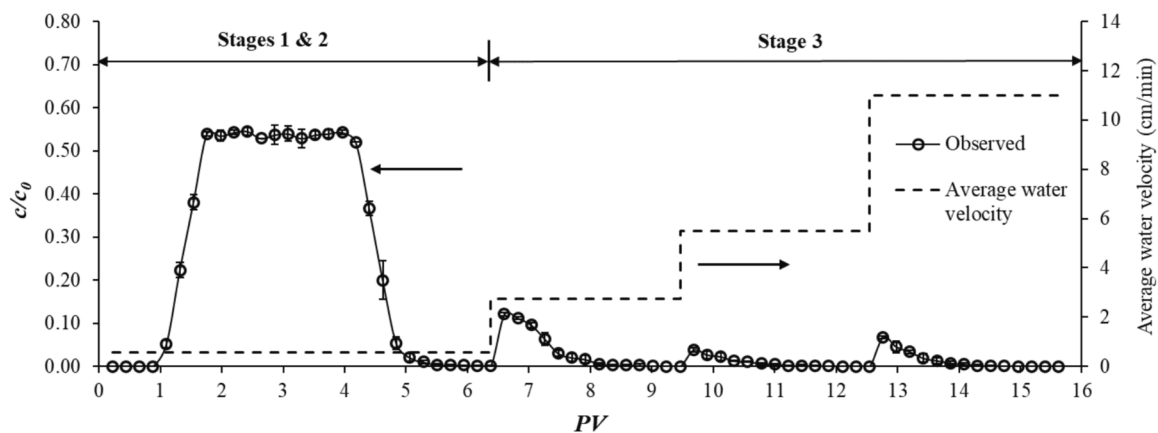


Fig. 3. Observed breakthrough curve of CML colloids for experiment 3. Average water velocity variation is shown on the secondary y-axis. Ionic strength was 25 mM.

supported this hypothesis (modeled data not presented). Moreover, the comparison of colloid retention profiles at the end of stages 2 and 3 of experiments 1, 2, and 3 reveals that in stage 3, colloids were remobilized from near the column inlet, but were redeposited downstream near the column outlet (Fig. 5). This was also observed by Zhang et al. (2015). The step increases in velocity did not release any colloids when the ionic strength was 10 mM (Fig. 4) as the retained particle mass at the end of stage 2 was much less than experiments 1–3 (Table 3). Hence, fewer

colloids were available for release during temporal variations in flow in stage 3 for experiment 4. This is supported by similar colloid retention profiles at the end of stages 2 and 3 for experiment 4 in Fig. 5 which shows that the velocity variations didn't have any significant impact on the retention profile at the end of stage 3, and the retained colloidal mass was almost uniformly distributed throughout the soil column. This implies colloid retention predominantly in low velocity regions at 10 mM (Du et al., 2013; Torkzaban et al., 2010). Increase in velocity will not

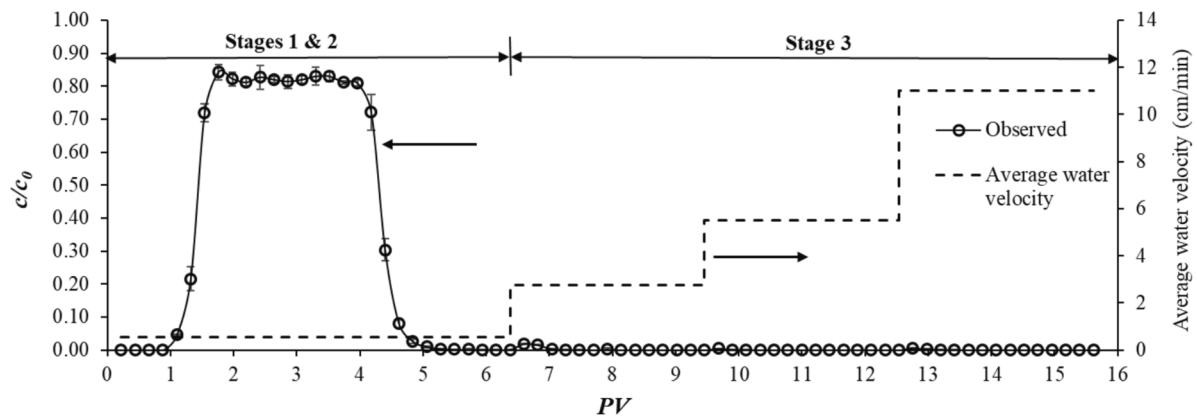


Fig. 4. Observed breakthrough curve of CML colloids for experiment 4. Average water velocity variation is shown on the secondary y-axis. Ionic strength was 10 mM.

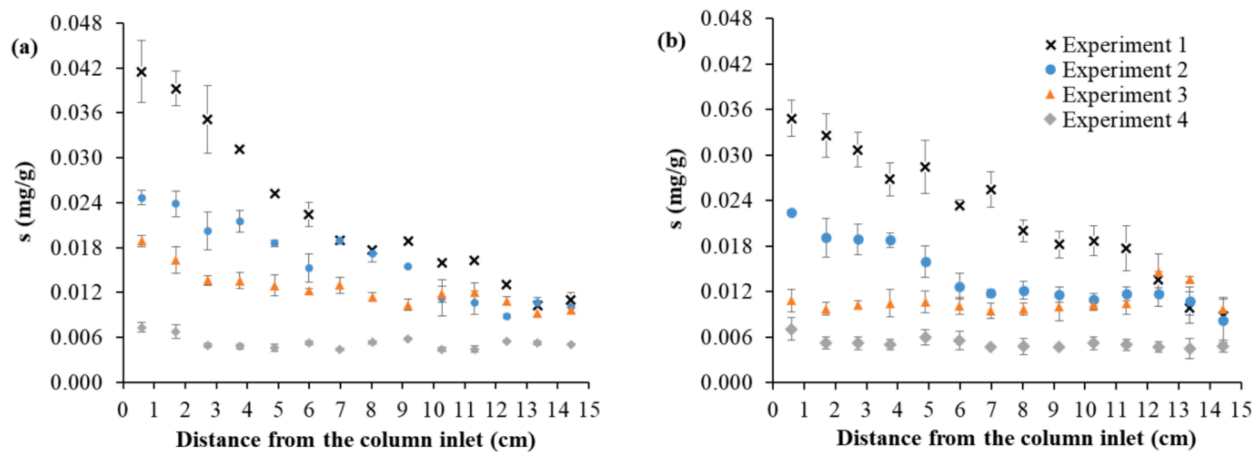


Fig. 5. Colloid retention profile at the end of (a) stage 2 and (b) stage 3 of experiments 1–4. Ionic strength was 100, 50, 25, and 10 mM in experiments 1, 2, 3 and 4, respectively.

Table 3
Experimental mass balance information for experiments 1–4.

Experiment no.	Ionic strength (mM)	Stages 1 & 2		Stage 3				
		M_{eluted}^a (%)	$M_{retained}^b$ (%)	Step 1	Step 2	Step 3	Total M_{eluted}^c (%)	Total $M_{retained}^d$ (%)
1	100	20.41	79.59	0.06	0.14	0.15	0.35	79.33
2	50	43.75	56.25	1.72	0.66	1.56	3.94	51.67
3	25	55.39	44.61	2.90	0.84	1.28	5.02	38.47
4	10	79.18	20.82	0.23	0.04	0.06	0.33	18.44

^a Percentage mass eluted during stages 1 and 2.

^b Percentage mass retained inside the column at the end of stage 2 obtained from colloid retention profile.

^c Percentage mass eluted during stage 3.

^d Percentage mass retained inside the column at the end of stage 3 obtained from colloid retention profile.

alter the hydrodynamic torque acting on colloids retained in low velocity regions. As a result, we did not observe any significant release during velocity increases in stage 3 of experiment 4 (Fig. 4).

Our results clearly show that the effect of temporal variations in average water velocity on remobilization of deposited colloids is ionic-strength dependent (Figs. 1–4), with the highest release occurring at an ionic strength of 25 mM (Table 3). Also, Figs. 1–4 show that the highest release at any ionic strength occurred during the first step-increase in average water velocity, i.e., from 0.55 to 2.75 cm/min, except for experiment 1. Table 3 shows that significant mass of deposited colloids was still retained in the soil at the end of stage 3 in all the four experiments. This indicates the minimal effect of temporal variations in velocity on remobilization of deposited colloids. The fractional

release of deposited colloids during any step-increase in average water velocity depends on the spatial variation of the hydrodynamic and adhesive torques in the 3D pore space of the soil acting on the deposited colloids (Bergendahl and Grasso, 2000; Torkzaban et al., 2015). Colloids will be released from grain surfaces where hydrodynamic torque exceeds the adhesive torque and vice versa. Negligible release of deposited colloids during stage 3 in experiments 1–4 (Figs. 1–4 and Table 3) indicates very large adhesive torque between the colloids and grains that could not be overcome by the hydrodynamic torque caused by velocity increase. Surface roughness and charge heterogeneity of the soil grains are known to have significant effects on the magnitudes of adhesive and hydrodynamic torques (Bergendahl and Grasso, 2000; Bradford and Torkzaban, 2013; Shen et al., 2012), and thereby on the colloid release

behavior during temporal variations in velocity. Surface roughness of the soil grains decreases the energy barrier, thereby favoring primary minimum deposition leading to increased adhesive torque and immobilization (Bradford and Torkzaban, 2013). Moreover, roughness reduces the local flow velocity near the grain surface between the protrusions, thereby reducing the hydrodynamic torque. Hence, the particles attached between the protrusions may not get detached due to velocity increase (Zhang et al., 2015). Also, colloids deposited at flow stagnation zones may not get released due to increase in flow velocity (Bradford and Bettahar, 2006; Du et al., 2013; Johnson et al., 2007; Torkzaban et al., 2010).

The observations from this study are consistent with the experimental results at the column scale (Bergendahl and Grasso, 2000; Torkzaban et al., 2015; Zhang et al., 2012) and pore scale (Zhang et al., 2015). Torkzaban et al. (2015) observed negligible release of natural colloids from consolidated sandstone samples during temporal increase in velocity from 8 m/d to 100 m/d due to injection of native ground water. However, in the same experiment, a spike release of deposited colloids was observed with each step-increase in velocity when, instead of native groundwater, desalinated water was used. The reason behind this release was due to the low ionic strength of reverse osmosis water leading to small adhesive torque which could be easily overcome by increasing hydrodynamic torques due to temporal increase in velocity. However, only a small fraction of deposited colloids was released upon each subsequent step-increase in flow velocity, and the fraction of released colloids decreased with increase in the number of step-increases in velocity (Torkzaban et al., 2015). Similar distributed release of deposited colloids was also observed by Bergendahl and Grasso (2000) and Zhang et al. (2015), who reported that the hydrodynamic forces are spatially variable due to the complex pore structure of the porous media and roughness of the grain surfaces, and there exists a critical hydrodynamic shear force at each velocity which allows only a fraction of the deposited colloids to get detached. Also, some studies observed decreased release of colloids with increase in the duration of flow interruption due to increased deposition caused by gravity settling and diffusion, and colloid aggregation and subsequent straining in pore throats (Carstens et al., 2017; Wang et al., 2016; Zhang et al., 2012). Hence, it can be concluded from the above discussion that reattachment of released colloids in the downstream reach of the column is an important mechanism and might be the reason behind the negligible release of colloids in the effluent during stage 3 in experiments 1–4.

3.2. Colloid remobilization due to simultaneous temporal variations in velocity and ionic strength

Colloid breakthrough curves for experiments 5–8 are given in Figs. 6–9, respectively. Colloid retention profiles in soil at the end of stages 2 and 3 of experiments 5–8 are given in Fig. 10a and b, respectively. The mass balance information for the above experiments along with the mass released during every step-change in velocity and ionic strength is given in Table 4. For comparison, we have also included in Figs. 6–9 the observed breakthrough curves of CML colloids during temporal variations in ionic strength alone as reported in Krishna et al. (2022). The simulated ionic strength variations at the outlet of the column obtained by solving advection–dispersion equation as reported in Krishna et al. (2022) are also shown in Figs. 6–9. Figs. 6–9 show that the colloid release curves during stage 3 were characterized by sharp peaks followed by long tails. The release curve for each simultaneous step-change in velocity and ionic strength was either unimodal or bimodal depending on the deposition ionic strength in stages 1 & 2 (Figs. 6–9). In experiment 5, we did three simultaneous variations of velocity and ionic strength followed by three step decrease of ionic strength while velocity is kept constant (Fig. 6). In all cases we observed a single spike for every step-change in flow and/or ionic strength, and the peak coincided with the time of arrival of the ionic-strength front at the column outlet (Fig. 6). Fig. 6 shows that the instantaneous colloid release in the effluent due to increasing velocity is negligible for experiment 5 as there is no spike in concentration at the instant of velocity increase. Fig. 6 also indicates that the colloid release behavior during simultaneous temporal variations in flow and ionic strength is similar to that of temporal variations in ionic strength alone, with the peak concentration being larger for the simultaneous temporal variations in flow and ionic strength than the ionic-strength only case. The increased release during simultaneous temporal variations in flow and ionic strength is caused by a greater hydrodynamic torque exerted on attached particles due to larger velocities combined with reduced adhesive torque due to ionic strength reductions.

Figs. 7 and 8 show that in experiments 6 and 7, for each simultaneous step-change in velocity and ionic strength, we get two distinct spikes; one corresponding to the instant of increase of flow velocity and the second one corresponding to the time of arrival of ionic strength front at the outlet. This becomes evident from comparing Figs. 7 and 8 to the corresponding release curves obtained during temporal variations in

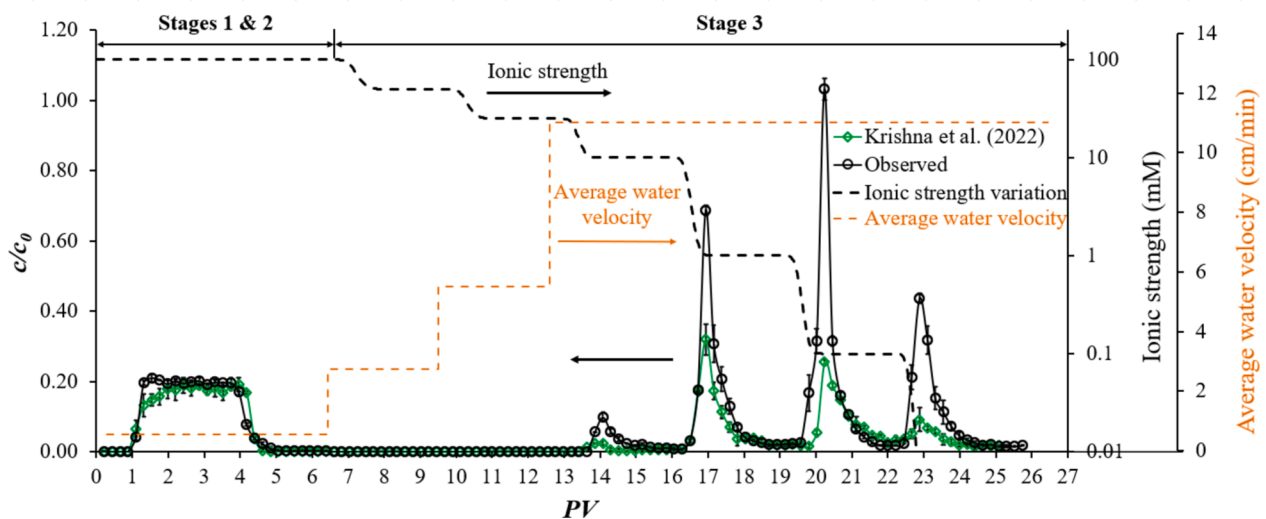


Fig. 6. Observed breakthrough curves of CML colloids for experiment 5 (black circles) and the corresponding experimental results during temporal variations in ionic strength alone plotted from Krishna et al. (2022) (green diamonds). Average water velocity and simulated ionic strength variations at the outlet of the column as reported in Krishna et al. (2022) are shown on the secondary y-axis. (For interpretation of the references to colour in this figure legend, the reader is referred to the web version of this article.)

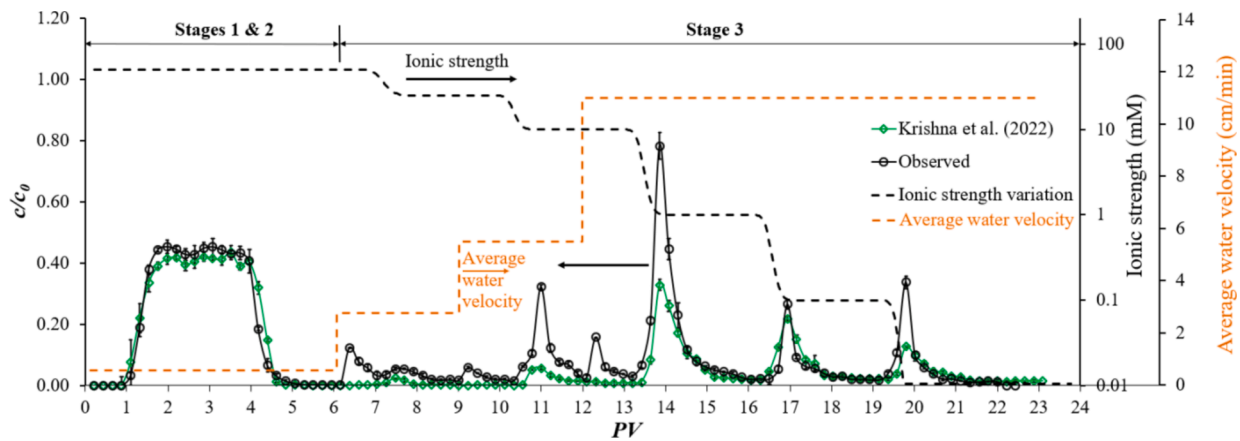


Fig. 7. Observed breakthrough curve of CML colloids for experiment 6 (black circles) and corresponding experimental results during temporal variations in ionic strength alone plotted from Krishna et al. (2022) (green diamonds). Average water velocity and simulated ionic strength variations at the outlet of the column as reported in Krishna et al. (2022) are shown on the secondary y-axis. (For interpretation of the references to colour in this figure legend, the reader is referred to the web version of this article.)

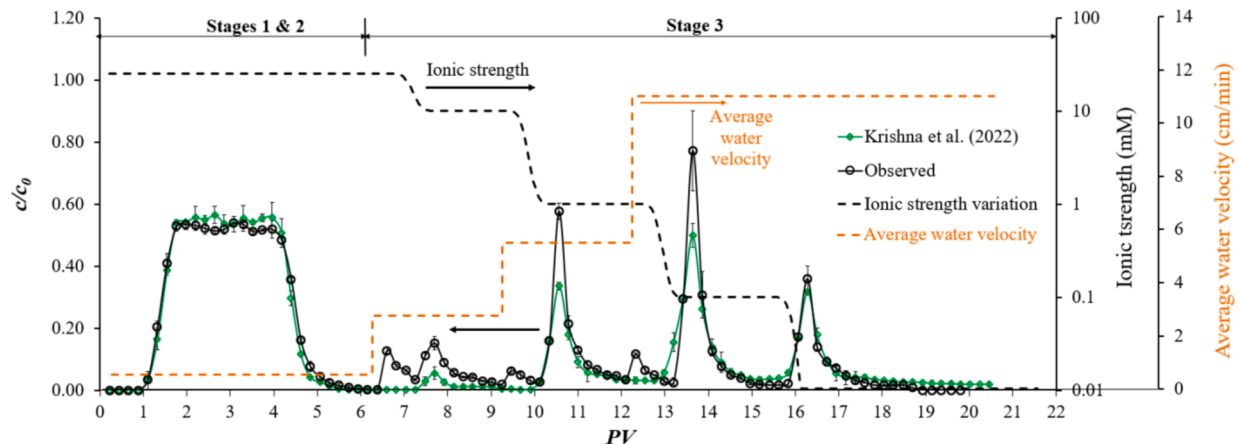


Fig. 8. Observed breakthrough curve of CML colloids for experiment 7 (black circles) and corresponding experimental results during temporal variations in ionic strength alone plotted from Krishna et al. (2022) (green diamonds). Average water velocity and simulated ionic strength variations at the outlet of the column as reported in Krishna et al. (2022) are shown on the secondary y-axis. (For interpretation of the references to colour in this figure legend, the reader is referred to the web version of this article.)

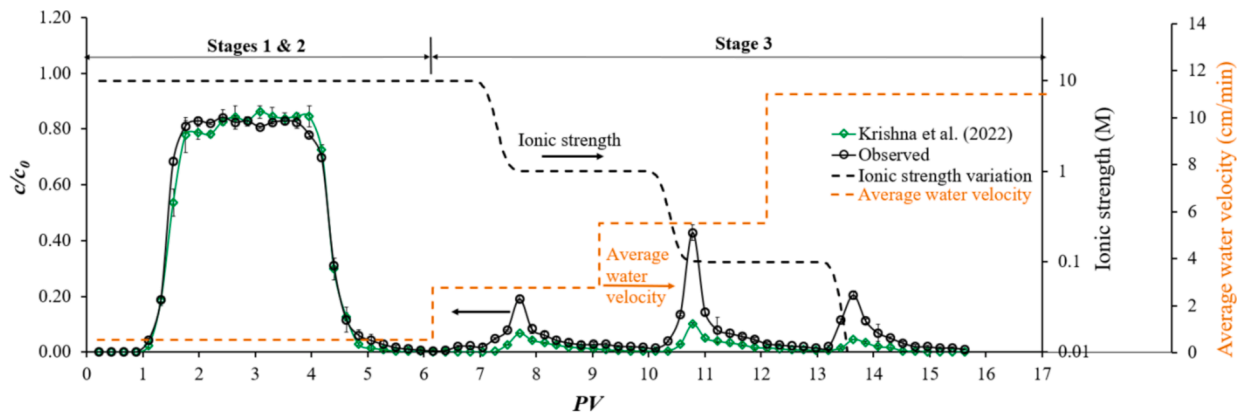


Fig. 9. Observed breakthrough curve of CML colloids for experiment 8 (black circles) and corresponding experimental results during temporal variations in ionic strength alone plotted from Krishna et al. (2022) (green diamonds). Average water velocity and simulated ionic strength variations at the outlet of the column as reported in Krishna et al. (2022) are shown on the secondary y-axis. (For interpretation of the references to colour in this figure legend, the reader is referred to the web version of this article.)

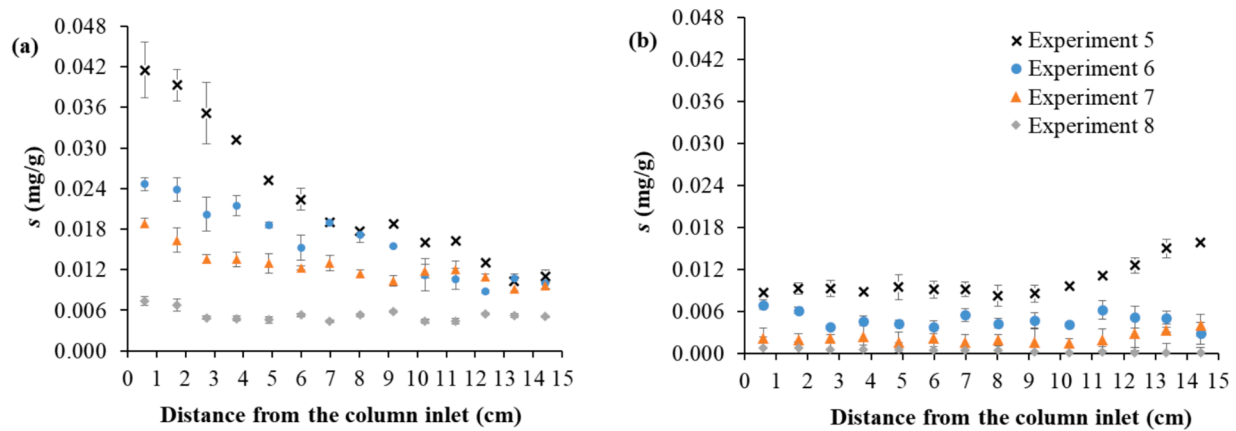


Fig. 10. Colloid retention profiles for CML colloids at the end of (a) stage 2, and (b) stage 3 for experiments 5–8.

Table 4

Experimental mass balance information for experiments 5–8.

Experiment No.	Stages 1 and 2				Stage 3							
	Average water velocity (cm/min)	Ionic strength (mM)	M_{eluted}^a (%)	$M_{retained}^b$ (%)	Step 1	Step 2	Step 3	Step 4	Step 5	Step 6	Total M_{eluted}^c (%)	Total $M_{retained}^d$ (%)
5	0.55	100	19.95	80.05	0.00	0.00	2.32	11.37	15.12	11.52	40.33	38.71
6	0.55	50	40.82	59.18	3.92	7.78	17.41	5.29	6.69	–	41.09	16.78
7	0.55	25	53.80	46.20	6.05	10.27	13.39	7.49	–	–	37.20	7.83
8	0.55	10	79.39	20.61	5.01	8.48	5.61	–	–	–	19.10	1.32

^a Percentage mass eluted during stages 1 and 2.

^b Percentage mass retained inside the column at the end of stage 2 calculated using colloid retention profile.

^c Percentage mass eluted during stage 3.

^d Percentage mass retained inside the column at the end of stage 3 calculated using colloid retention profile.

flow alone (Figs. 2 and 3) and temporal variations in ionic-strength alone ((experimental results of Krishna et al. (2022) presented as green diamonds in Fig. 6). The magnitudes of the first peaks in Figs. 7 and 8 for every step-change in flow and ionic strength are similar to those in Figs. 2 and 3, respectively. This indicates that the ionic strength variation in each step for experiments 6 and 7 does not contribute to the first spike in the release curve which was caused by velocity increase alone. This is because the increase in velocity is instantaneous throughout the column whereas the change in ionic strength is gradual. Hence, the adhesive torque remains unaltered during the instant of flow variations and when the hydrodynamic torque on particles becomes larger than the adhesive torque, they get released into the bulk fluid. However, the magnitude of second peak in the release curves during simultaneous temporal variations is greater than those during temporal variations in ionic strength alone (green data points in Figs. 7 and 8). This is because a larger hydrodynamic torque, exerted on particles due to increased velocity, together with smaller adhesive torque, due to decreased ionic strength, drives more release of particles from grain surfaces.

The colloid release curve for experiment 8 (Fig. 9) is characterized by a single spike for every step-change in flow velocity and ionic strength, with the peak occurring during the passage of the ionic strength front at the column outlet. Unlike experiments 6 and 7 (Figs. 7 and 8), but similar to experiment 5 (Fig. 6), there was no instantaneous release due to flow variations in experiment 8 (Fig. 9). This release behavior is similar to that for temporal variations in flow alone at 10 mM ionic strength (experiment 4 and Fig. 4), where no release was observed during step-increases in flow velocity.

Experiments 5–8 (Figs. 6–9) show that for every step-change in velocity and/or ionic strength, the peak in the release curve caused by the passage of the ionic-strength front is higher than the peak caused by velocity increase. Also, results show that simultaneous temporal

variations in flow and chemistry (experiments 5–8, Figs. 6–9) released more colloids than temporal variations in ionic strength alone (Figs. 6–9) and temporal variations in flow velocity alone (experiments 1–4, Figs. 1–4). Weak adhesive forces due to ionic strength reduction coupled with higher hydrodynamic drag due to increased velocity are the cause of more release of colloids during simultaneous temporal variations in flow and chemistry. Figs. 6–9 show that significant release of deposited colloids occurred when the ionic strength was reduced to below 10 mM. However, the critical value of ionic strength, i.e., the ionic strength below which the release is significant, is velocity-dependent, and hence, will take different values for different experiments (experiments 5–8). We hypothesize that the critical value of ionic strength due to simultaneous temporal variations in flow and chemistry to be larger than that due to ionic strength reduction alone (7.48 mM as found in Krishna et al. (2022)). Further, Table 4 shows that the percentage of retained colloids released in stage 3 increased with decreasing ionic strength in stages 1 and 2. The corresponding values are 50.4 %, 69.4 %, 80.5 %, and 92.6 % for experiments 5–8, respectively. These results are in line with the colloid retention profile at the end of stage 3 shown in Fig. 10 which represents larger retention for experiment 5, when the colloids were deposited at a high ionic strength of 100 mM during stages 1 and 2. Moreover, significant mass of injected colloids, 40 % and 20 %, was still retained in soil at the end of stage 3 for experiments 5 and 6, respectively (Table 4). Fig. 10 shows that the retained mass of colloids for experiment 5 is greater near the outlet than the inlet. This might be due to re-deposition of the colloids released near the inlet in the downstream region. More colloid retention at the outlet was also observed for experiment 7 where the colloids were deposited at an ionic strength of 25 mM during stages 1 and 2.

A balance of hydrodynamic and adhesive torques acting on attached colloids is essential to explain the partial release of deposited colloids during various steps in stage 3 for experiments 5–8. The torque balance

performed by calculating adhesive torque using interaction energy profile obtained from DLVO theory (Fig. S1) and hydrodynamic torque by assuming a smooth collector and average water velocity could not explain the partial release of colloids observed during stage 3 (data not shown). This is because the DLVO theory assumes the particles and grains to be uniformly charged (Redman et al., 2004; Shani et al., 2008; Johnson and Hilpert, 2013) and hence, the effect of grain surface roughness and charge heterogeneity on adhesive torque is not accounted for. Also, calculation of hydrodynamic torque by assuming the collector to be a uniformly-shaped smooth sphere cannot account for the spatial variation in the average water velocity in soil. The incomplete release of retained colloids from soil during stage 3 is potentially due to the effect of surface roughness and charge heterogeneity of the sand grains, as well as colloid retention in flow stagnation zones. The sand surface has both convex and concave regions, which play a crucial role in colloid deposition and release (Li et al., 2017; Shen et al., 2015). The velocity is low in concave regions, and the colloids deposited there do not get remobilized even when ionic strength is decreased and/or velocity is increased (Li et al., 2017). However, the colloids that were retained at the top of the convex asperities can get easily detached due to perturbations in flow and chemistry. This is because the convex asperities significantly reduce the depth of the primary minimum, thereby reducing the adhesive torque of colloids at grain surfaces (Li et al., 2017, 2020; Shen et al., 2015, 2018). Also, particles retained at the flow stagnation zones would not get affected by velocity variations. Thus, the complex interplay between surface roughness and surface charge heterogeneity plays critical roles in the retention and release of colloids during temporal variations in flow and chemistry. Other factors that can cause spatial variations in hydrodynamic torque are pore-size distribution of sand, pore connectivity and pore-shape variations (Bergendahl and Grasso 2000; Bradford and Torkzaban, 2013; Li et al., 2017, 2020; Shen et al., 2015, 2018; Zhang et al., 2015). Hence, detailed experimental and modeling studies at pore scale are essential to understand the mechanisms behind the observed release during simultaneous temporal variations in flow and chemistry.

4. Summary and conclusions

In this study, first we investigated the effect of temporal variations in flow alone, and then simultaneous temporal variations in flow velocity and ionic strength on remobilization of deposited colloids in saturated porous media through laboratory column experiments. Four experiments, each at a different ionic strength (100, 50, 25, and 10 mM), were performed to study the effect of temporal step increases in velocity on colloid remobilization. An instantaneous spike release of colloids followed by a long tail was observed with every step-increase in average water velocity for 50 and 25 mM, with the peak coinciding with the instant of velocity increase. However, negligible colloid release was observed in the effluent for ionic strengths of 100 and 10 mM. The instantaneous sharp release of colloids might be due to a distance-dependent exponential increase in colloid release rate, with the greatest release occurring at the column outlet. The effect of temporal variations in velocity on remobilization of deposited colloids is ionic-strength dependent with the highest release occurring at an ionic strength of 25 mM. Experimental results showed minimal effect of temporal variations in velocity on remobilization of deposited colloids with significant mass retained in the soil at the end of all the experiments. The fractional release of deposited colloids during temporal variations in velocity depends on the spatial distribution of the hydrodynamic and adhesive torques acting on the deposited colloids, which in turn are affected by pore-size distribution, pore connectivity, grain roughness, and charge heterogeneity of soil grains. It is also found that the remobilized colloids from near the inlet were redeposited in the downstream regions, leading to negligible release in the effluent.

The colloid release curves due to simultaneous temporal variations in flow and ionic strength were characterized by sharp peaks followed by

long tails. The release curve for every step-change in velocity and ionic strength was unimodal for deposition ionic strengths of 100 and 10 mM and coincided with the instant of arrival of the ionic-strength front at the column outlet. However, the release curve for every step-change in velocity and ionic strength was bimodal for deposition ionic strengths of 50 and 25 mM, with the first peak coinciding with the instant of increase in flow velocity and a second delayed spike coinciding with the passage of the ionic strength front. Temporal variations in both flow and ionic strength released more colloids in the effluent than temporal variations in ionic-strength alone or temporal variations in flow velocity alone. The increased release during simultaneous temporal variations in flow and chemistry is due to the coupling of greater hydrodynamic torque exerted on attached particles due to larger velocities with the smaller adhesive torque due to ionic strength reductions. However, significant mass was still retained in soil at the end of all experiments. The incomplete release of retained colloids from soil during simultaneous temporal variations in flow and ionic strength might be due to the effect of surface roughness and charge heterogeneity of the sand grains, and colloid retention in flow stagnation zones. The amount of colloids released during simultaneous temporal variations in flow and ionic strength depends on the temporal and spatial variations in the hydrodynamic and adhesive torques acting on the attached colloids. Transient flow and chemistry conditions result in temporal variations in hydrodynamic and adhesive torques, respectively, acting on attached colloids. Pore-size distribution, pore connectivity, and grain surface roughness lead to spatial variations in hydrodynamic torque acting on the attached colloids whereas charge heterogeneity and surface roughness of soil grains causes spatial variations in adhesive torque acting on attached colloids. A calculation of hydrodynamic and adhesive torques performed by assuming smooth uniformly-charged spherical grains could not explain the partial release of colloids during temporal variations. Hence, experimental and modeling studies at pore scale are essential to unravel the mechanisms behind the observed release during combined temporal variations in flow and chemistry.

CRedit authorship contribution statement

Yerramilli Sai Rama Krishna: Conceptualization, Methodology, Validation, Formal analysis, Investigation, Writing – original draft. **N. Seetha:** Conceptualization, Methodology, Writing – review & editing, Supervision, Funding acquisition. **S. Majid Hassanizadeh:** Writing – review & editing, Conceptualization.

Declaration of competing interest

The authors declare that they have no known competing financial interests or personal relationships that could have appeared to influence the work reported in this paper.

Acknowledgements

The authors acknowledge the funding received from Science and Engineering Research Board (SERB), Government of India (sanction no. VJR/2020/000006) for carrying out this work. SMH acknowledges support from Deutsche Forschungsgemeinschaft (DFG, German Research Foundation) under Germany's Excellence Strategy - EXC 2075 - 390740016 and from the Stuttgart Center for Simulation Science (SimTech).

Appendix A. Supplementary data

Supplementary data to this article can be found online at <https://doi.org/10.1016/j.jhydrol.2024.132144>.

Data availability

Data will be made available on request.

References

- Akhtar, N., Syakir Ishak, M.I., Bhawani, S.A., Umar, K., 2021. Various natural and anthropogenic factors responsible for water quality degradation: a review. *Water* 13 (19), 2660.
- Auset, M., Keller, A.A., Brissaud, F., Lazarova, V., 2005. Intermittent filtration of bacteria and colloids in porous media. *Water Resour. Res.* 41 (9), 1–13. <https://doi.org/10.1029/2004WR003611>.
- Bergendahl, J., Grasso, D., 2000. Prediction of colloid detachment in a model porous media: hydrodynamics. *Chem. Eng. Sci.* 55 (9), 1523–1532.
- Bhuvankar, P., Cihan, A., Birkholzer, J., 2022. Pore-scale CFD simulations of clay mobilization in natural porous media due to fresh water injection. *Chem. Eng. Sci.* 247. <https://doi.org/10.1016/j.ces.2021.117046>.
- Bradford, S.A., Bettahar, M., 2006. Concentration dependent transport of colloids in saturated porous media. *J. Contam. Hydrol.* 82 (1–2), 99–117.
- Bradford, S.A., Kim, H., 2012. Causes and implications of colloid and microorganism retention hysteresis. *J. Contam. Hydrol.* 138, 83–92.
- Bradford, S.A., Torkzaban, S., 2013. Colloid interaction energies for physically and chemically heterogeneous porous media. *Langmuir* 29, 3668–3676. <https://doi.org/10.1021/la400229f>.
- Bradford, S.A., Torkzaban, S., Leij, F., Simunek, J., 2015. Equilibrium and kinetic models for colloid release under transient solution chemistry conditions. *J. Contam. Hydrol.* 181, 141–152. <https://doi.org/10.1016/j.jconhyd.2015.04.003>.
- Carrard, N., Foster, T., Willetts, J., 2019. Groundwater as a source of drinking water in southeast Asia and the Pacific: a multi-country review of current reliance and resource concerns. *Water* 11 (8), 1605.
- Carstense, J.F., Bachmann, J., Neuweiler, I., 2017. Effects of flow interruption on transport and retention of iron oxide colloids in quartz sand. *Colloids Surf. A Physicochem. Eng. Asp.* 520 (February), 532–543. <https://doi.org/10.1016/j.colsurfa.2017.02.003>.
- Du, Y., Shen, C., Zhang, H., Huang, Y., 2013. Effects of flow velocity and nonionic surfactant on colloid straining in saturated porous media under unfavorable conditions. *Transp. Porous Media* 98 (1), 193–208.
- El-Farhan, Y.H., DeNovio, N.M., Herman, J.S., Hornberger, G.M., 2000. Mobilization and transport of soil particles during infiltration experiments in an agricultural field, Shenandoah Valley, Virginia. *Environ. Sci. Technol.* 34 (17), 3555–3559.
- Fang, J., Xu, M.j., Wang, D.j., Wen, B., Han, J.y., 2013. Modeling the transport of TiO₂ nanoparticle aggregates in saturated and unsaturated granular media: effects of ionic strength and pH. *Water Res.* 47 (3), 1399–1408. <https://doi.org/10.1016/j.watres.2012.12.005>.
- Johnson, W.P., Hilpert, M., 2013. Upscaling colloid transport and retention under unfavorable conditions: linking mass transfer to pore and grain topology. *Water Resour. Res.* 49 (9), 5328–5341.
- Johnson, W.P., Li, X., Yal, G., 2007. Colloid retention in porous media: mechanistic confirmation of wedging and retention in zones of flow stagnation. *Environ. Sci. Tech.* 41 (4), 1279–1287.
- Karunanidhi, D., Aravinthasamy, P., Subramani, T., Kumar, M., 2021. Human health risks associated with multipath exposure of groundwater nitrate and environmental friendly actions for quality improvement and sustainable management: a case study from Texvalley (Tiruppur region) of India. *Chemosphere* 265, 129083.
- Kermani, M.S., Jafari, S., Rahnama, M., Raoof, A., 2020. Direct pore scale numerical simulation of colloid transport and retention. Part I: fluid flow velocity, colloid size, and pore structure effects. *Adv. Water Resour.* 144, 103694.
- Krishna, Y.S.R., Seetha, N., Hassanizadeh, S.M., 2022. Experimental and numerical investigation of the effect of temporal variation in ionic strength on colloid retention and remobilization in saturated porous media. *J. Contam. Hydrol.* 251, 104079.
- Lapworth, D.J., Baran, N., Stuart, M.E., Ward, R.S., 2012. Emerging organic contaminants in groundwater: a review of sources, fate and occurrence. *Environ. Pollut.* 163, 287–303.
- Lenhart, J.J., Saiers, J.E., 2003. Colloid mobilization in water-saturated porous media under transient chemical conditions. *Environ. Sci. Tech.* 37 (12), 2780–2787. <https://doi.org/10.1021/es025788v>.
- Li, T., Jin, Y., Huang, Y., Li, B., Shen, C., 2017. Observed dependence of colloid detachment on the concentration of initially attached colloids and collector surface heterogeneity in porous media. *Environ. Sci. Tech.* 51 (5), 2811–2820. <https://doi.org/10.1021/acs.est.6b06264>.
- Li, P., Karunanidhi, D., Subramani, T., Srinivasamoorthy, K., 2021. Sources and consequences of groundwater contamination. *Arch. Environ. Contam. Toxicol.* 80, 1–10.
- Li, T., Shen, C., Wu, S., Jin, C., Bradford, S.A., 2020. Synergies of surface roughness and hydration on colloid detachment in saturated porous media: column and atomic force microscopy studies. *Water Res.* 183, 116068.
- Liang, Y., Zhou, J., Dong, Y., Klumpp, E., Šimůnek, J., Bradford, S.A., 2020. Evidence for the critical role of nanoscale surface roughness on the retention and release of silver nanoparticles in porous media. *Environ. Pollut.* 258, 113803. <https://doi.org/10.1016/j.envpol.2019.113803>.
- Mishra, S., Tiwary, D., Ohri, A., Agnihotri, A.K., 2019. Impact of Municipal Solid Waste Landfill leachate on groundwater quality in Varanasi, India. *Groundw. Sustain. Develop.* 9, 100230.
- Mukhopadhyay, R., Sarkar, B., Khan, E., Alessi, D.S., Biswas, J.K., Manjaiah, K.M., Ok, Y. S., 2022. Nanomaterials for sustainable remediation of chemical contaminants in water and soil. *Crit. Rev. Environ. Sci. Technol.* 52 (15), 2611–2660.
- Nishad, S., Al-Raoush, R.I., Alazaiza, M.Y.D., 2021. Release of colloids in saturated porous media under transient hydro-chemical conditions: a pore-scale study. *Colloids Surf. A Physicochem. Eng. Asp.* 614 (December 2020). <https://doi.org/10.1016/j.colsurfa.2021.126188>.
- Nocito-Gobel, J., Tobiasson, J.E., 1996. Effects of ionic strength on colloid deposition and release. *Colloids Surf. A Physicochem. Eng. Asp.* 107, 223–231.
- Pazmino, E., Trauscht, J., Johnson, W.P., 2014. Release of colloids from primary minimum contact under unfavorable conditions by perturbations in ionic strength and flow rate. *Environ. Sci. Tech.* 48 (16), 9227–9235. <https://doi.org/10.1021/es502503y>.
- Ramesh, K., Elango, L., 2012. Groundwater quality and its suitability for domestic and agricultural use in Tondiar river basin, Tamil Nadu, India. *Environ. Monit. Assess.* 184, 3887–3899.
- Redman, J.A., Walker, S.L., Elimelech, M., 2004. Bacterial adhesion and transport in porous media: Role of the secondary energy minimum. *Environmental science & technology* 38 (6), 1777–1785. <https://doi.org/10.1021/es034887l>.
- Sadeghi, G., Schijven, J.F., Behrends, T., Hassanizadeh, S.M., Gerritse, J., Kleingeld, P.J., 2011. Systematic study of effects of pH and ionic strength on attachment of phage PRD1. *Groundwater* 49 (1), 12–19.
- Shen, C., Li, B., Huang, Y., Jin, Y., 2007. Kinetics of coupled primary-and secondary-minimum deposition of colloids under unfavorable chemical conditions. *Environ. Sci. Tech.* 41 (20), 6976–6982.
- Shen, C., Lazouskaya, V., Zhang, H., Wang, F., Li, B., Jin, Y., Huang, Y., 2012. Theoretical and experimental investigation of detachment of colloids from rough collector surfaces. *Colloids Surf. A Physicochem. Eng. Asp.* 410, 98–110. <https://doi.org/10.1016/j.colsurfa.2012.06.025>.
- Shen, C., Zhang, M., Zhang, S., Wang, Z., Zhang, H., Li, B., Huang, Y., 2015. Influence of surface heterogeneities on reversibility of fullerene (nC60) nanoparticle attachment in saturated porous media. *J. Hazard. Mater.* 290, 60–68.
- Shani, C., Weisbrod, N., Yakirevich, A., 2008. Colloid transport through saturated sand columns: Influence of physical and chemical surface properties on deposition. *Colloids and Surfaces A: Physicochemical and Engineering Aspects* 316 (1–3), 142–150.
- Shen, C., Bradford, S.A., Li, T., Li, B., Huang, Y., 2018. Can nanoscale surface charge heterogeneity really explain colloid detachment from primary minima upon reduction of solution ionic strength? *J. Nanopart. Res.* 20 (6). <https://doi.org/10.1007/s11051-018-4265-8>.
- Singh, K.P., Malik, A., Mohan, D., Singh, V.K., Sinha, S., 2006. Evaluation of groundwater quality in northern Indo-Gangetic alluvium region. *Environ. Monit. Assess.* 112, 211–230.
- Torkzaban, S., Bradford, S.A., 2016. Critical role of surface roughness on colloid retention and release in porous media. *Water Res.* 88, 274–284.
- Torkzaban, S., Bradford, S.A., Vanderzalm, J.L., Patterson, B.M., Harris, B., Prommer, H., 2015. Colloid release and clogging in porous media: effects of solution ionic strength and flow velocity. *J. Contam. Hydrol.* 181, 161–171. <https://doi.org/10.1016/j.jconhyd.2015.06.005>.
- Torkzaban, S., Kim, H.N., Simunek, J., Bradford, S.A., 2010. Hysteresis of colloid retention and release in saturated porous media during transients in solution chemistry. *Environmental science & technology* 44 (5), 1662–1669.
- Tosco, T., Tiraferri, A., Sethi, R., 2009. Ionic strength dependent transport of microparticles in saturated porous media: modeling mobilization and immobilization phenomena under transient chemical conditions. *Environ. Sci. Tech.* 43 (12), 4425–4431.
- Wang, Y., Bradford, S.A., Shang, J., 2020. Release of colloidal biochar during transient chemical conditions: the humic acid effect. *Environ. Pollut.* 260, 114068. <https://doi.org/10.1016/j.envpol.2020.114068>.
- Wang, Z., Wang, D., Li, B., Wang, J., Li, T., Zhang, M., Shen, C., 2016. Detachment of fullerene nC60 nanoparticles in saturated porous media under flow/stop-flow conditions: column experiments and mechanistic explanations. *Environ. Pollut.* 213, 698–709.
- Wang, H., Zhang, W., Zeng, S., Shen, C., Jin, C., Huang, Y., 2019. Interactions between nanoparticles and fractal surfaces. *Water Res.* 151, 296–309. <https://doi.org/10.1016/j.watres.2018.12.029>.
- Zhang, L., Hou, L., Wang, L., Kan, A.T., Chen, W., Tomson, M.B., 2012. Transport of fullerene nanoparticles (nC60) in saturated sand and sandy soil: controlling factors and modeling. *Environ. Sci. Tech.* 46 (13), 7230–7238.
- Zhang, Q., Raoof, A., Hassanizadeh, S.M., 2015. Pore-scale study of flow rate on colloid attachment and remobilization in a saturated micromodel. *J. Environ. Qual.* 44 (5), 1376–1383.
- Zhou, D., Wang, D., Cang, L., Hao, X., Chu, L., 2011. Transport and re-entrainment of soil colloids in saturated packed column: effects of pH and ionic strength. *J. Soil. Sediment.* 11, 491–503.
- Zhuang, J., McCarthy, J.F., Tyner, J.S., Perfect, E., Flury, M., 2007. In situ colloid mobilization in Hanford sediments under unsaturated transient flow conditions: effect of irrigation pattern. *Environ. Sci. Tech.* 41 (9), 3199–3204. <https://doi.org/10.1021/es062757h>.